Effective spin-chain model for strongly interacting one-dimensional atomic gases with an arbitrary spin

Lijun Yang and Xiaoling Cui*

Beijing National Laboratory for Condensed Matter Physics, Institute of Physics, Chinese Academy of Sciences, Beijing 100190, People's Republic of China

(Received 25 October 2015; published 19 January 2016)

We present a general form of the effective spin-chain model for strongly interacting atomic gases with an arbitrary spin in one-dimensional (1D) traps. In particular, for high-spin systems the atoms can collide in multiple scattering channels, and we find that the resulting form of spin-chain model generically follows the same structure as that of the interaction potentials. This is a unified form working for any spin, statistics (Bose or Fermi), and confinement potentials. We adopt the spin-chain model to reveal both the ferromagnetic (FM) and antiferromagnetic (AFM) magnetic orders for strongly interacting spin-1 bosons in 1D traps. We further show that by adding the spin-orbit coupling, the FM and AFM orders can be gradually destroyed and eventually the ground state exhibits universal spin structure and contacts that are independent of the strength of spin-orbit coupling.

DOI: 10.1103/PhysRevA.93.013617

I. INTRODUCTION

A strongly interacting system is known to be notoriously difficult to solve in physics. There is one exception, however, for the infinite coupling of a one-dimensional (1D) system that the exact solutions of bosons and fermions can be constructed by taking advantage of the peculiar feature of femionalization [1–5]. In cold-atom experiments, strongly interacting Tonks-Girardeau gases have been realized in both spinless bosons [6–8] and spin-$\frac{1}{2}$ fermions [9–11]. A fascinating property with an infinite coupling (hard-core interaction) is that the ground states of a spinful system are highly degenerate and their wave functions share the form of

$$\Psi(x_1,\mu_1;\ldots;x_N,\mu_N) = \phi_F(x_1,\ldots,x_N)\psi(x_1,\mu_1;\ldots;x_N,\mu_N). \quad (1)$$

Here x_i and μ_i are the position and spin of the ith particle ($i = 1,\ldots,N$) and ϕ_F is the Slater determinant made up of the lowest N level of eigenstates in the 1D system, a common factor of all degenerate wave functions Ψ. While the energy of Ψ is solely given by ϕ_F, the ψ part uniquely describes the distribution of spins in the coordinate space and determines the degeneracy of the system. The large degeneracy has been shown to facilitate the ferromagnetic transition of spin-$\frac{1}{2}$ fermions by tuning the coupling strength across this critical point [12,13].

Apart from the infinite-coupling case, it is interesting and also more practical to learn about the physics in the regime of large but finite couplings. This regime is more realistic to achieve in experiments, which can be adiabatically connected to the noninteracting limit by tuning the interaction strength. With finite couplings, the magnetic properties of bosons and fermions are very different. General theorems have shown that the ground state for spin-$\frac{1}{2}$ fermions is with the lowest total spin [14], while for isospin-$\frac{1}{2}$ bosons is is ferromagnetic [15–17]. Accordingly, the effective antiferromagnetic (AFM) and ferromagnetic (FM) spin-spin exchange interactions have been successfully extracted from the Bethe-ansatz solutions of strongly coupling spin-$\frac{1}{2}$ fermions [18] and bosons [19]. Recently, taking advantage of the high controllability of a few particles in trapped ultracold systems [9,10], a number of studies have revealed the energy spectra and correlation effects for a few spin-$\frac{1}{2}$ fermions by numerical simulations [20–23]. In the strong-coupling regime, an effective Heisenberg spin-chain model has also been deduced [24–27]. The resulting antiferromagnetic correlation has recently been confirmed through the tunneling measurement of a few spin-$\frac{1}{2}$ fermions in 1D traps [28]. Moreover, the effective models for spin-$\frac{1}{2}$ bosons [29,30] and for higher-spin cases with SU(N) symmetry [24,25] have also been discussed.

In this work we present a general form of the effective spin-chain model for strongly interacting trapped atomic gases with an arbitrary spin and arbitrary statistics (Bose or Fermi). In particular, for high-spin atomic systems, the multichannel interactions can break the SU(N) symmetry and the ground state can have a wide variety of magnetic orders, including FM, AFM, or even intriguing ones, depending on the relative coupling strength between different scattering channels. We find that the resulting form of effective spin-chain model generically follows the same structure as that of the interaction potentials classified by scattering channels and thus respects the symmetry of the original Hamiltonian for trapped systems. This form can be applied to any spin value, Bose or Fermi statistics, and confinement potentials. Taking the strongly interacting spin-1 bosons as an example, we adopt the effective spin-chain model and reveal both FM and AFM correlations by choosing different interaction strengths for different cold atoms.

Based on the spin-chain model, we further study the effect of spin-orbit coupling (SOC), which has been realized in cold-atom experiments by two-photon Raman processes [31–36]. For spin-1 bosons, we show how the FM or AFM correlations are destroyed with increasing SOC strength. In the SOC-dominated regime, we obtain universal spin texture and contacts, which are independent of the actual SOC strength. These results are consistent with previous studies on the spin-orbit-coupled spin-$\frac{1}{2}$ fermions at infinite coupling [37,38].

*xlcui@iphy.ac.cn

The rest of the paper is organized as follows. In Sec. II we present the derivation of the effective spin-chain model with an arbitrary spin. We take the spin-$\frac{1}{2}$ (two-component) fermions and bosons as a starting point to get insight into the general structure of spin-chain models with an arbitrary spin. In Sec. III, based on the effective spin-chain model, we study the system of spin-1 bosons and show the ground state exhibiting FM or AFM correlations. We further study the interplay effect of strong interactions and SOC to the ground-state properties of spin-1 bosons under the effective spin-chain model. We summarize in Sec. IV.

II. EFFECTIVE SPIN-CHAIN MODEL

We first write the noninteracting Hamiltonian for atoms confined in the 1D trap ($\hbar$ is set to unity throughout the paper):

$$H_0 = \sum_i \left(-\frac{1}{2m}\frac{\partial^2}{\partial x_i^2} + V_T(x_i) \right). \tag{2}$$

Here V_T is a spin-independent trapping potential and in this paper we consider a harmonic trap with trapping frequency ω_T and characteristic length $a_T = 1/\sqrt{m\omega_T}$. The interaction is generally characterized by the coupling constant g, and for the high-spin atoms there can be multiple scattering channels with multiple coupling constants. In this work we consider the large repulsive coupling constants in all scattering channels, which can be achieved through the confinement-induced resonance [39] or the preparation of very dilute gas.

The basic idea for the construction of an effective spin-chain model is that the physics in the vicinity of infinite coupling $g \to \infty$ can be well deduced from the known $g = \infty$ limit, by treating $1/g$ as a small parameter in the framework of the perturbation theory. In this way the wave function to the zeroth order of $1/g$ can be approximated as a certain superposition of degenerate states at $1/g = 0$, which leads to an energy functional up to the linear $1/g$ and gives the effective model. This idea has been successfully applied to the spin-$\frac{1}{2}$ fermion case and leads to the AFM Heisenberg spin-chain model therein [24–27].

In this section we will give a detailed introduction to the degenerate ground states at infinite coupling, as they are essential for the construction of the spin-chain model when slightly away from this special point. These degenerate states are classified by the order of spins in coordinate space and thus are referred to as the spin-ordered states as in Ref. [37]. Using these states, we will rederive the spin-chain model for the spin-$\frac{1}{2}$ fermions and bosons as a starting point. Finally, we will extend our derivation to an arbitrary spin case and present a general form of the spin-chain model for both fermions and bosons.

A. Spin-ordered state

To conveniently enumerate the degenerate ground states at infinite coupling of 1D systems, we define the spin-ordered state

$$|\{\xi_1,\xi_2,\ldots,\xi_N\}\rangle \equiv |\vec{\xi}\rangle. \tag{3}$$

In this state, a sequence of spins $\xi_1, \xi_2, \ldots, \xi_N$ is placed in order in the 1D coordinate space. Explicitly, its wave function is written as

$$\langle x_1,\ldots,x_N;\mu_1,\ldots,\mu_N|\vec{\xi}\rangle = \sum_P \theta(x_{P_1},x_{P2},\ldots,x_{P_N}) \prod_i \delta_{\xi_i,\mu_{P_i}}, \tag{4}$$

where P is a permutation of the integers $(1,2,\ldots,N)$ and

$$\theta(x_{P_1},x_{P2},\ldots,x_{P_N}) = 1 \quad \text{if } x_{P_1} < x_{P2} < \cdots < x_{P_N}$$
$$= 0 \quad \text{otherwise.} \tag{5}$$

The spin-ordered state as defined in (3) is symmetric under the simultaneous change of the coordinate and spin of any two particles. It is then straightforward to construct the degenerate ground states of bosons and fermions at infinite coupling using this class of states:

$$\Psi_B^{\xi} = |\phi_F(x_1,x_2,\ldots,x_N)|\langle x_1,\ldots,x_N;\mu_1,\ldots,\mu_N|\vec{\xi}\rangle, \tag{6}$$

$$\Psi_F^{\xi} = \phi_F(x_1,x_2,\ldots,x_N)\langle x_1,\ldots,x_N;\mu_1,\ldots,\mu_N|\vec{\xi}\rangle, \tag{7}$$

where Ψ_B (Ψ_F) is the wave function of bosons (fermions) obeying Bose (Fermi) statistics and ϕ_F is the Slater determinant composed by the lowest N level of eigenstates of H_0 in Eq. (2),

$$\phi_F(x_1,x_2,\ldots,x_N) = \frac{1}{\sqrt{N!}} D(x_1,x_2,\ldots,x_N)$$
$$= \prod_{i<j}(x_i - x_j) F(x_1,x_2,\ldots,x_N), \tag{8}$$

with $F(\{x_i\})$ a fully symmetric function (with respect to the exchange of any two coordinates). In Eqs. (6) and (7), the ϕ_F part determines the ground-state energy of the system, while the ξ part uniquely determines the spin distribution or order of the system. By considering different spin orders in ξ, one can cover all the degenerate ground states at infinite coupling. Moreover, it is easy to check that the states with different spin orders are orthogonal to each other. Therefore, the wave functions (6) and (7) constitute a complete and orthogonal basis set in the ground-state manifold of particles with infinite-coupling strength.

Given Eqs. (6) and (7), one can compute the particle density at the ith spin order

$$n_i(x) = \int d\mathbf{x}|D|^2\theta(x_1,x_2,\ldots,x_i,\ldots,x_N)\delta(x - x_i), \tag{9}$$

where $d\mathbf{x} = \prod_{i=1}^N dx_i$, $n_i(x)$ gives the probability of finding the ith-order particle at position x, and we have $\int dx\, n_i(x) = 1$. In Fig. 1 we show $n_i(x)$ (with $i = 1,2,\ldots,N$) for $N = 6$ particles in a 1D harmonic trap. It is found that the density peak for each spin order is well separated from each other and $n_i(x)$ can be well approximated by a Gaussian function [37]

$$n_i(x) \to \frac{1}{\sqrt{\pi}\sigma_i} e^{-(x-\bar{x}_i)^2/\sigma_i^2}, \tag{10}$$

where $\bar{x}_i = \int x n_i(x) dx$ is the average location of the ith particle and σ_i is the width of the density distribution for the ith particle, which can be obtained by fitting $n_i(x)$ with the above function. In Table I we present the result of x_i, $\bar{x}_{i+1} - \bar{x}_i$, and σ_i for $N = 4,6,8$ particles. It is found that the neighboring $\bar{x}_i$

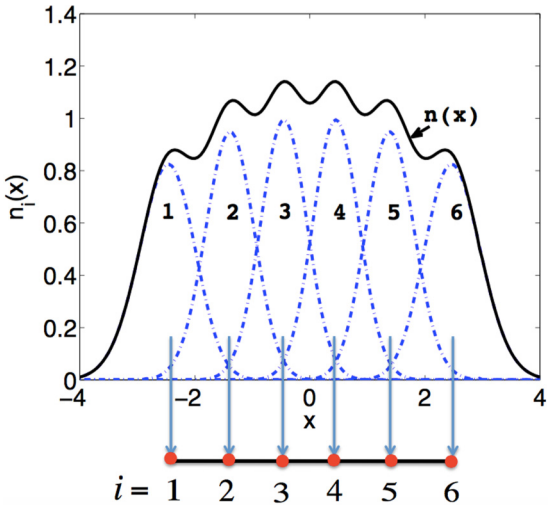

FIG. 1. Particle density $n_i(x)$ (blue dashed lines) for $N = 6$ particles in a harmonic trap. Here x and n_i are in the unit of a_T and $1/a_T$, respectively, with a_T the confinement length of the trapping potential. The black curve shows the total density $n(x) \equiv \sum_i n_i(x)$. The spin-order index i is mapped to the site index i in the effective spin-chain model.

and $\bar{x}_{i+1}$ are nearly equally spaced by a distance d and each σ_i is typically of order d and varies little for different i.

When limited to the ground-state manifold, we can map the spin-order index i to the site index i and thus the physics with the spin-ordered state can be mapped to that under an effective spin-chain model. Here we would like to point out an essential difference between the effective spin chain and the real lattice configuration: The particle density at each site of the effective spin chain can actually spread over the interparticle spacing of atoms in the Harmon trap [40], while in the real lattice case it is just localized around each lattice site. The large spreading in the effective spin-chain case can lead to strong interference of spins between neighboring orders and give rise to exotic spin-density profiles [37].

TABLE I. Averaged location $\bar{x}_i$, difference $\bar{x}_{i+1} - \bar{x}_i$, and variance σ_i for $N = 4,6,8$. All lengths are in the unit of a_T.

i	$\bar{x}_i$	$\bar{x}_{i+1} - \bar{x}_i$	σ_i
	$N = 4$		
1	−1.751	1.200	0.739
2	−0.551	1.102	0.653
3	0.551	1.200	0.653
4	1.751		0.739
	$N = 6$		
1	−2.451	0.985	0.684
2	−1.466	1.016	0.595
3	−0.450	0.900	0.567
4	0.450	1.016	0.567
5	1.466	0.985	0.595
6	2.451		0.684
	$N = 8$		
1	−3.049	1.005	0.648
2	−2.044	0.855	0.556
3	−1.189	0.795	0.522
4	−0.394	0.780	0.508
5	0.394	0.795	0.508
6	1.189	0.855	0.522
7	2.044	1.005	0.556
8	3.049		0.648

B. Effective spin-chain model for the spin-$\frac{1}{2}$ system

In this section we derive the spin-chain model for the spin-$\frac{1}{2}$ system, which was previously studied in Refs. [24–27,29,30]. Here we adopt a systematic method for easy generalization to the high-spin case. For the spin-$\frac{1}{2}$ system with a total particle number of $N = N_\uparrow + N_\downarrow$, the number of different spin-ordered states, i.e., the ground-state degeneracy at infinite coupling, is $N_{\rm dg} = N!/N_\uparrow!N_\downarrow!$.

1. *Spin-$\frac{1}{2}$ fermions*

Due to Fermi statistics, the contact interaction for spin-$\frac{1}{2}$ fermions only occurs in the spin-singlet channel with coupling constant g. In fact, in this case one can directly write the interaction as

$$U = g \sum_{i<j} \delta(x_i - x_j), \tag{11}$$

because the particles scattering in other channels (other than the spin singlet) will be automatically ruled out by the Fermi statistics.

For large g (and thus small $1/g$), the many-body wave function can be written as a certain superposition of the degenerate ground states (7) at $1/g = 0$,

$$\Psi(\{x_i\};\{\mu_i\}) = \phi_F(\{x_i\}) \sum_{k=1}^{N_{\rm dg}} a_k \langle \{x_i\};\{\mu_i\}|\vec{\xi}_k\rangle, \tag{12}$$

with $\{a_k\}$ the coefficient of the spin-ordered state $|\vec{\xi}_k\rangle$ ($k = 1,\ldots,N_{\rm dg}$). At small $1/g$, the energy can be expanded as

$$E = E_0 - \frac{\kappa}{g}, \tag{13}$$

where E_0 is the degenerate energy at $1/g = 0$ (determined by ϕ_F) and κ is proportional to Tan's contact in one dimension [42]:

$$\kappa = \frac{\partial E}{\partial(-1/g)} = g^2 \frac{\partial E}{\partial g}. \tag{14}$$

In the following we aim at expressing κ in terms of the coefficients $\{a_k\}$ in Eq. (12), which is essential to the construction of the effective spin-chain model.

Applying the Hellmann-Feynman theorem [43] to Eq. (14), we obtain

$$\begin{aligned}\kappa &= \lim_{g\to\infty} g^2 \int d\mathbf{x} \sum_{i<j} \delta(x_i - x_j)|\Psi(\{x_i\};\{\mu_i\})|^2 \\ &= \frac{N(N-1)}{2} \lim_{g\to\infty} g^2 \int d\mathbf{x}\, \delta(x_i - x_j)|\Psi(\{x_i\};\{\mu_i\})|^2.\end{aligned} \tag{15}$$

The integral in this equation can be obtained by considering the Schrödinger equation

$$\left(-\sum_{k\neq i,j}\frac{1}{2m}\frac{\partial^2}{\partial x_k^2}+g\sum_{(k,l)\neq(i,j)}\delta(x_k-x_l)+\sum_k V_T(x_k)\right.$$
$$\left.-\frac{1}{4m}\frac{\partial^2}{\partial X_{ij}^2}-\frac{1}{m}\frac{\partial^2}{\partial x_{ij}^2}+g\delta(x_{ij})\right)\Psi(\{x_i\};\{\mu_i\})=0, \tag{16}$$

where $x_{ij}=x_i-x_j$ and $X_{ij}=(x_i+x_j)/2$ represent, respectively, the relative and center-of-mass motions of i and j. The boundary condition around $x_{ij}=0$ gives

$$\frac{1}{m}\left(\frac{\partial\Psi}{\partial x_{ij}}\bigg|_{x_{ij}=0^+}-\frac{\partial\Psi}{\partial x_{ij}}\bigg|_{x_{ij}=0^-}\right)=g\Psi|_{x_{ij}=0}. \tag{17}$$

So we get κ in Eq. (15) as

$$\kappa=\frac{N(N-1)}{2}\left(\frac{1}{m}\right)^2\int d\mathbf{x}\left|\frac{\partial\Psi}{\partial x_{ij}}\bigg|_{x_{ij}=0^-}^{x_{ij}=0^+}\right|^2. \tag{18}$$

Given the property of ϕ_F in Eq. (8), κ can be further reduced to

$$\kappa=\frac{N(N-1)}{2}\left(\frac{1}{m}\right)^2\int d\mathbf{x}\left|\frac{\partial\phi_F}{\partial x_{ij}}\bigg|_{x_{ij}=0}\right|^2$$
$$\times\left|\sum_{k=1}^{N_{\rm dg}}a_k(\{\{x_i\};\{\mu_i\}|\vec{\xi}_k\rangle|_{x_{ij}=0^+}-\langle\{x_i\};\{\mu_i\}|\vec{\xi}_k\rangle|_{x_{ij}=0^-})\right|^2. \tag{19}$$

Note that the right-hand side this equation is an $(N-1)$-fold integration due to the constraint $x_{ij}=0$.

With the inclusion of $\frac{\partial\phi_F}{\partial x_{ij}}$, it is easy to check that only when the two coordinates x_i and x_j stay in the neighboring order in the wave function can they contribute to κ. Assume x_i and x_j stay in the lth and $(l+1)$st order in Ψ; we denote their contribution to κ by κ_l. For two particles there are four spin-ordered states

$$|\{\uparrow\uparrow\}\rangle,\quad |\{\uparrow\downarrow\}\rangle,\quad |\{\downarrow\uparrow\}\rangle,\quad |\{\downarrow\downarrow\}\rangle, \tag{20}$$

which can form one singlet and three triplets

$$|00\rangle_{l,l+1}=\frac{|\{\uparrow\downarrow\}\rangle-|\{\downarrow\uparrow\}\rangle}{\sqrt{2}},$$
$$|11\rangle_{l,l+1}=|\{\uparrow\uparrow\}\rangle,$$
$$|10\rangle_{l,l+1}=\frac{|\{\uparrow\downarrow\}\rangle+|\{\downarrow\uparrow\}\rangle}{\sqrt{2}},$$
$$|1,-1\rangle_{l,l+1}=|\{\downarrow\downarrow\}\rangle.$$

According to the definition of spin-ordered states in Eq. (4), the above states can be simplified as

$$|00\rangle_{l,l+1}\to\frac{|\uparrow_i\downarrow_j\rangle-|\downarrow_i\uparrow_j\rangle}{\sqrt{2}}[\theta(x_i,x_j)-\theta(x_j,x_i)],$$
$$|11\rangle_{l,l+1}\to|\uparrow_i\uparrow_j\rangle,$$
$$|10\rangle_{l,l+1}\to\frac{|\uparrow_i\downarrow_j\rangle+|\downarrow_i\uparrow_j\rangle}{\sqrt{2}},$$
$$|1,-1\rangle_{l,l+1}\to|\downarrow_i\downarrow_j\rangle.$$

It is then easy to see that only the singlet state $|00\rangle$ can contribute to κ_l in Eq. (19). Physically, this is due to the Fermi statistics and the asymmetric feature of the fermionic wave function (12).

As the spin-ordered states in the wave function (12) can be classified according to the total spin and total magnetization of the lth- and $(l+1)$st-order particles, we can write

$$\sum_k a_k|\vec{\xi}_k\rangle\to\sum_n a_n^{SM}|SM\rangle_{l,l+1}|\vec{\xi}_n'\rangle, \tag{21}$$

where $|SM\rangle$ can be $|00\rangle$, $|11\rangle$, $|10\rangle$, or $|1,-1\rangle$ and $\vec{\xi}'$ denotes the spin-ordered states for the other order numbers except l and $l+1$. Based on (21), we can obtain κ_l as

$$\kappa_l=\frac{N!}{2}\left(\frac{1}{m}\right)^2\int d\mathbf{x}\left|\frac{\partial\phi_F}{\partial x_{ij}}\bigg|_{x_{ij}=0}\right|^2\theta(\cdots<x_i=x_j<\cdots)$$
$$\times\sum_n|2a_n^{00}|^2, \tag{22}$$

where x_i is at the lth order in the θ function (i.e., there are $l-1$ particles with coordinates smaller than x_i). The contribution of these two order numbers (l and $l+1$) to the energy (13) is (up to a constant E_0)

$$E_l=-\frac{\kappa_l}{g}. \tag{23}$$

Now we construct an effective spin-chain model by replacing the spin-order index with the lattice site index in Eq. (21). In order to obtain the same energy functional as (23), we must consider the effective Hamiltonian

$$H_l=-\frac{J_l}{g}P_{00}(l,l+1), \tag{24}$$

where $P_{00}(l,l+1)$ is the projection operator for neighboring sites (l and $l+1$) forming a singlet and J_l follows

$$J_l=2N!\left(\frac{1}{m}\right)^2\int d\mathbf{x}\left|\frac{\partial\phi_F}{\partial x_{ij}}\bigg|_{x_{ij}=0}\right|^2\theta(\cdots<x_i=x_j<\cdots). \tag{25}$$

By expanding $P_{00}(l,l+1)$ in terms of the Pauli matrix and also noting that the total Hamiltonian is the summation of all neighboring-pair contributions $H_{\rm eff}=\sum_l H_l$, finally we arrive at the effective spin-chain model for spin-$\frac{1}{2}$ fermions:

$$H_{\rm eff}=\sum_l\frac{J_l}{g}\left(\mathbf{s}_l\cdot\mathbf{s}_{l+1}-\frac{1}{4}\right). \tag{26}$$

The result of an antiferromagnetic correlation in the above Hamiltonian is consistent with the Lieb-Mattis theorem, which

states that the ground state of spin-$\frac{1}{2}$ fermions is with the lowest total spin [14], as well as the indication from Bethe-ansatz solutions [18].

2. *Spin-$\frac{1}{2}$ bosons*

For two-component (with pseudospins $\uparrow,\downarrow$) bosons, the interaction can occur in three channels

$$U = \sum_{\sigma=\uparrow,\downarrow} g_{\sigma\sigma} \sum_{i<j} \delta(x_{i\sigma} - x_{j\sigma}) + g_{\uparrow\downarrow} \sum_{i,j} \delta(x_{i\uparrow} - x_{j\downarrow}). \quad (27)$$

These channels actually represent three spin-triplet channels due to the Bose statistics.

For large $g_{\sigma\sigma'}$, the many-body wave function can be written as a certain superposition of the degenerate ground states [Eq. (7)] at all $1/g_{\sigma\sigma'} = 0$,

$$\Psi(\{x_i\};\{\mu_i\}) = |\phi_F(\{x_i\})| \sum_{k=1}^{N_{\rm dg}} a_k \langle\{x_i\};\{\mu_i\}|\vec{\xi}_k\rangle, \quad (28)$$

where the wave function is distinguished from Eq. (12) by replacing ϕ_F with its absolute value. This replacement will significantly affect the expression of $\kappa_{\sigma\sigma'}$ as defined in the energy expansion at small $1/g_{\sigma\sigma'}$:

$$E = E_0 - \frac{\kappa_{\uparrow\uparrow}}{g_{\uparrow\uparrow}} - \frac{\kappa_{\downarrow\downarrow}}{g_{\downarrow\downarrow}} - \frac{\kappa_{\uparrow\downarrow}}{g_{\uparrow\downarrow}}, \quad (29)$$

with $\kappa_{\sigma\sigma'}$ given by

$$\kappa_{\sigma\sigma'} = \frac{\partial E}{\partial(-1/g_{\sigma\sigma'})} = g_{\sigma\sigma'}^2 \frac{\partial E}{\partial g_{\sigma\sigma'}}. \quad (30)$$

Following a procedure similar to that in the preceding section, we obtain $\kappa_{\sigma\sigma'}$ as

$$\kappa_{\uparrow\uparrow} = \frac{N(N-1)}{2}\left(\frac{1}{m}\right)^2 \int d\mathbf{x} \left|\frac{\partial\phi_F}{\partial x_{ij}}\Big|_{x_{ij}=0}\right|^2 \left|\sum_{k=1}^{N_{\rm dg}} a_k \delta_{\mu_i,\uparrow}\delta_{\mu_j,\uparrow}(\langle\{x_i\};\{\mu_i\}|\vec{\xi}_k\rangle|_{x_{ij}=0^+} + \langle\{x_i\};\{\mu_i\}|\vec{\xi}_k\rangle|_{x_{ij}=0^-})\right|^2, \quad (31)$$

$$\kappa_{\downarrow\downarrow} = \frac{N(N-1)}{2}\left(\frac{1}{m}\right)^2 \int d\mathbf{x} \left|\frac{\partial\phi_F}{\partial x_{ij}}\Big|_{x_{ij}=0}\right|^2 \left|\sum_{k=1}^{N_{\rm dg}} a_k \delta_{\mu_i,\downarrow}\delta_{\mu_j,\downarrow}(\langle\{x_i\};\{\mu_i\}|\vec{\xi}_k\rangle|_{x_{ij}=0^+} + \langle\{x_i\};\{\mu_i\}|\vec{\xi}_k\rangle|_{x_{ij}=0^-})\right|^2, \quad (32)$$

$$\kappa_{\uparrow\downarrow} = N(N-1)\left(\frac{1}{m}\right)^2 \int d\mathbf{x} \left|\frac{\partial\phi_F}{\partial x_{ij}}\Big|_{x_{ij}=0}\right|^2 \left|\sum_{k=1}^{N_{\rm dg}} a_k \delta_{\mu_i,\uparrow}\delta_{\mu_j,\downarrow}(\langle\{x_i\};\{\mu_i\}|\vec{\xi}_k\rangle|_{x_{ij}=0^+} + \langle\{x_i\};\{\mu_i\}|\vec{\xi}_k\rangle|_{x_{ij}=0^-})\right|^2. \quad (33)$$

Again we select two coordinates x_i and x_j to stay in the neighboring orders, the lth and $(l+1)$st, in the wave function and denote their contribution to $\kappa_{\sigma\sigma'}$ by $\kappa_{\sigma\sigma';l}$. After simple algebra, we find that only the three triplets can contribute; explicitly, $|11\rangle_{l,l+1}$, $|1,-1\rangle_{l,l+1}$, and $|1,0\rangle_{l,l+1}$ contribute to $\kappa_{\uparrow\uparrow}$, $\kappa_{\downarrow\downarrow}$, and $\kappa_{\uparrow\downarrow}$, respectively. By rewriting the spin-ordered state in the same form as in Eq. (21), we can then obtain

$$\kappa_{\uparrow\uparrow;l} = J_l \sum_n |a_n^{11}|^2, \quad (34)$$

$$\kappa_{\uparrow\downarrow;l} = J_l \sum_n |a_n^{10}|^2, \quad (35)$$

$$\kappa_{\downarrow\downarrow;l} = J_l \sum_n |a_n^{1,-1}|^2, \quad (36)$$

where J_l follows the same expression as Eq. (25). Considering the energy functional (29) and replacing the spin-ordered index in (21) as the lattice site index, we can write the effective spin-chain model as

$$H_{\rm eff} = -\sum_l J_l \left(\frac{1}{g_{\uparrow\uparrow}} P_{11}(l,l+1) + \frac{1}{g_{\downarrow\downarrow}} P_{1,-1}(l,l+1) + \frac{1}{g_{\uparrow\downarrow}} P_{10}(l,l+1)\right), \quad (37)$$

with $P_{SM}(l,l+1)$ the projection operator for neighboring sites l and $l+1$ forming a triplet with $S=1$ and $M=0,\pm1$. For the case of $g_{\uparrow\uparrow} = g_{\downarrow\downarrow} \equiv g$, Eq. (37) can be reduced to the XXZ Heisenberg model

$$H_{\rm eff} = \sum_l J_l \left[-\frac{1}{g_{\uparrow\downarrow}}\left(s_l^x s_{l+1}^x + s_l^y s_{l+1}^y\right) + \left(\frac{1}{g_{\uparrow\downarrow}} - \frac{2}{g}\right) s_l^z s_{l+1}^z - \left(\frac{1}{4g_{\uparrow\downarrow}} + \frac{1}{2g}\right)\right]. \quad (38)$$

For the case of the SU(2) interaction with spin-independent interaction strength $g_{\uparrow\uparrow} = g_{\downarrow\downarrow} = g_{\uparrow\downarrow} \equiv g$, Eq. (37) is reduced to the isotropic ferromagnetic Heisenberg model

$$H_{\rm eff} = -\sum_l \frac{J_l}{g}\left(\mathbf{s}_l \cdot \mathbf{s}_{l+1} + \frac{3}{4}\right). \quad (39)$$

This is consistent with general theorems showing that the ground state of isospin-$\frac{1}{2}$ bosons is ferromagnetic [15–17] and with the result from Bethe-ansatz solutions [19]. We note that the effective models (38) and (39) preserve the full symmetry of the original Hamiltonian, as they take the same structure as that of the interaction potentials. These models are related to those in Refs. [29,30] by a unitary transformation with the operator $u = \prod_{i=1}^{[N/2]} \sigma_i^z$ [44].

Comparing spin-$\frac{1}{2}$ bosons with fermions, we can see that the distinct correlations (FM for bosons and AFM for fermions) in Heisenberg Hamiltonians intrinsically result from the different symmetries allowed for the system. For the fermions, the antisymmetric feature of the wave function requires that the particles scatter in the singlet channel, while

for bosons the symmetric wave function requires the triplet channels. These scattering channels uniquely determine the structure of the effective models [see Eqs. (24) and (37)] in terms of the projector operators P_{SM}. This structure manifests the intrinsic relation between the statistics, the interaction channels, the effective spin-chain Hamiltonian, and the nature of the ground state. In the following we will show that it can be straightforwardly generalized to an arbitrary high-spin case.

C. Effective spin-chain model for a general spin

For a general high-spin system with multichannel scatterings, the interaction can be written as

$$U = \sum_{S=0}^{2f} \sum_{M=-S}^{S} g_{SM} \sum_{i<j} \delta(x_i - x_j) P_{SM}(i,j). \tag{40}$$

Here g_{SM} is the coupling constant for two particles scattering with total spin S and total magnetization M; $P_{SM}(i,j)$ is the projection operator for particles i and j scattering in the $\{SM\}$ sector.

For large g_{SM}, the many-body wave function of bosons B and fermions F can be written, respectively, as

$$\Psi_B(\{x_i\};\{\mu_i\}) = |\phi_F(\{x_i\})| \sum_k a_k \langle \{x_i\};\{\mu_i\}|\vec{\xi}_k\rangle, \tag{41}$$

$$\Psi_F(\{x_i\};\{\mu_i\}) = \phi_F(\{x_i\}) \sum_k a_k \langle \{x_i\};\{\mu_i\}|\vec{\xi}_k\rangle. \tag{42}$$

The energy expansion at small $1/g_{SM}$ can be expanded as

$$E = E_0 - \sum_{SM} \frac{\kappa_{SM}}{g_{SM}}, \tag{43}$$

with κ_{SM} given by

$$\kappa_{SM} = \frac{\partial E}{\partial(-1/g_{SM})} = g_{SM}^2 \frac{\partial E}{\partial g_{SM}}. \tag{44}$$

The boundary condition around $x_{ij} \equiv x_i - x_j = 0$ gives

$$\frac{1}{m} \frac{\partial (P_{SM}\Psi)}{\partial x_{ij}}\bigg|_{x_{ij}=0^-}^{x_{ij}=0^+} = g_{SM}(P_{SM}\Psi)|_{x_{ij}=0}, \tag{45}$$

with Ψ the many-body wave function for bosons or fermions. Based on this boundary condition, we can expand (44) as

$$\kappa_{SM} = \frac{N(N-1)}{2}\left(\frac{1}{m}\right)^2 \int d\mathbf{x} \left|\frac{\partial \phi_F}{\partial x_{ij}}\bigg|_{x_{ij}=0}\right|^2 \left|\sum_k a_k P_{SM}(\langle\{x_i\};\{\mu_i\}|\vec{\xi}_k\rangle|_{x_{ij}=0^+} - \langle\{x_i\};\{\mu_i\}|\vec{\xi}_k\rangle|_{x_{ij}=0^-})\right|^2 \tag{46}$$

for fermions and

$$\kappa_{SM} = \frac{N(N-1)}{2}\left(\frac{1}{m}\right)^2 \int d\mathbf{x} \left|\frac{\partial \phi_F}{\partial x_{ij}}\bigg|_{x_{ij}=0}\right|^2 \left|\sum_k a_k P_{SM}(\langle\{x_i\};\{\mu_i\}|\vec{\xi}_k\rangle|_{x_{ij}=0^+} + \langle\{x_i\};\{\mu_i\}|\vec{\xi}_k\rangle|_{x_{ij}=0^-})\right|^2 \tag{47}$$

for bosons. Assume two coordinates x_i and x_j stay in the neighboring orders, the lth and $(l+1)$st, in the wave function and denote their contribution to κ_{SM} by $\kappa_{SM;l}$. Due to the sign difference in the expressions of κ_{SM} for bosons and fermions, we find that only when the spin wave function in the spin-ordered states is symmetric for bosons and antisymmetric for fermions can it contribute to $\kappa_{SM;l}$. This can also select the spin channels in which the particles can scatter with each other.

By rewriting the spin-ordered state in the same form as in Eq. (21), we can obtain

$$\kappa_{SM;l} = J_l \sum_n |a_n^{SM}|^2, \tag{48}$$

where J_l follows the same expression as Eq. (25). Considering the energy functional (43) and replacing the spin-ordered index in (21) as the lattice site index, we can write the effective spin-chain model as

$$H_{\text{eff}} = -\sum_l J_l \sum_{SM} \frac{1}{g_{SM}} P_{SM}(l,l+1), \tag{49}$$

with $P_{SM}(l,l+1)$ the projection operator for neighboring sites l and $l+1$ forming a state with total spin S and total magnetization M. The above results can be easily applied to the spin-$\frac{1}{2}$ case of fermions ($S = M = 0$) and bosons ($S = 1, M = 0, \pm 1$) and accordingly the AFM or FM Heisenberg models can be obtained, respectively.

To this end, we have obtained a general form of effective spin-chain model (49) to describe strongly coupling atoms in a 1D trapped system. It can be applied for any statistics (Bose or Fermi), an arbitrary spin, and any spin-independent confinement potential. A key property of this effective model is that locally for each site l the Hamiltonian can be well separated into two parts: the coupling parameter J_l, which only relies on the local scattering amplitude, and the nearest-neighbor spin projection, which follows the same structure as the interaction model. This is closely related to the spin-charge separation in the wave function in the hard-core limit, as the form of Eqs. (41) and (42). More explicitly, the charge part ϕ_F determines the local scattering amplitude J_l, while the spin-ordered part together with the statistics determines the spin-relevant terms in Eq. (49).

III. STRONGLY COUPLING SPIN-1 BOSONS AND THE EFFECT OF SPIN-ORBIT COUPLING

In this section we apply the effective spin-chain model (49) to the spin-1 bosons. At low fields, the interaction of spin-1 bosons has SU(2) symmetry and can be classified into two channels

$$U = \sum_{i<j} \delta(x_i - x_j)[g_0 P_{S=0}(i,j) + g_2 P_{S=2}(i,j)], \tag{50}$$

where g_0 and g_2 are, respectively, the coupling constant in the total spin $S = 0$ and 2 channels [45,46] and P_S is the projection operator to the total spin S channel. Depending on the relative strength of g_0 and g_2, the cold-atom system can have an AFM (or polar or nematic) ground state (^{23}Na with $0 < g_0 < g_2$) or a FM ground state (^{87}Rb with $0 < g_2 < g_0$).

Based on the general formula (49), we can obtain the effective spin-chain model for spin-1 bosons in the strong-coupling limit

$$H_{\rm eff} = -\sum_l J_l\left(\frac{1}{g_0}P_0(l,l+1) + \frac{1}{g_2}P_2(l,l+1)\right), \quad (51)$$

which can be reduced to the form

$$H_{\rm eff} = -\frac{C_N}{g_0}\sum_l j_l[b_2(\mathbf{s}_l\cdot\mathbf{s}_{l+1})^2 + b_1\mathbf{s}_l\cdot\mathbf{s}_{l+1} + b_0], \quad (52)$$

with $\mathbf{s}_l$ the spin operator at site l. In writing this equation, J_l has been decomposed as the product of C_N and j_l; C_N is a quantity that only depends on the total particle number and the underlying trapping potential, which is proportional to the contact of the system, while the site dependence of J_l is simply included in j_l. Since j_l does not depend on the spin, here we use a good approximation derived for the spin-$\frac{1}{2}$ fermions case in a harmonic trap [27]

$$j_l = \frac{-(l-N/2)^2 + N^2/4}{N(N-1)/2} \quad (l = 1,\ldots,N-1). \quad (53)$$

In Eq. (52) b_2, b_1, and b_0 are dimensionless parameters depending on the ratio of interaction strengths in different channels

$$b_2 = \frac{1}{3}\left(1 + \frac{g_0}{2g_2}\right), \quad (54)$$

$$b_1 = \frac{g_0}{2g_2}, \quad (55)$$

$$b_0 = \frac{1}{3}\left(\frac{g_0}{g_2} - 1\right). \quad (56)$$

Note that the structure of the Hamiltonian (52) is the same as that of the bilinear-biquadratic isotropic quantum $S = 1$ chain and that in the Mott phase of spin-1 bosons in optical lattices [47–49]. The only difference is that here the coupling constants of neighbor spins are site dependent, due to the background trap potential and the resultant inhomogeneous particle (charge) density.

When we add the SOC to the system, which corresponds to a rotating field in the coordinate space [31–36]

$$H_{\rm SOC} = -\Omega_R\int dx \sum_{\sigma=0,-1}[e^{iqx}\psi^\dagger_\sigma(x)\psi_{\sigma+1}(x) + \text{H.c.}], \quad (57)$$

the spin texture and the spin-spin correlation according to $H_{\rm eff}$ [Eq. (52)] can be greatly modified. In the basis of spin-ordered states, the SOC Hamiltonian can be greatly reduced similarly to the spin-$\frac{1}{2}$ fermion case [37]. The single-particle term in $H_{\rm SOC}$ can be transformed to the on-site spin-flip term in an effective spin-chain Hamiltonian

$$H_{\rm SOC} = -\frac{1}{\sqrt{2}}\sum_{l=1}^{N}(\Omega_l s_{l-} + \text{H.c.}), \quad (58)$$

where $s_{l-} = \sqrt{2}(c^\dagger_{l,0}c_{l,1} + c^\dagger_{l,-1}c_{l,0})$ is the spin lowering operator at site l (with $c^\dagger_{l,\sigma}$ the creation operator of the spin-σ atom at site l) and the site-dependent coefficient is given by

$$\Omega_l = \Omega_R\int d\mathbf{x}\, N!|\phi_F|^2 e^{iqx_i}\theta(x_1,\ldots,x_i,\ldots,x_N), \quad (59)$$

where x_i is in the lth order in the θ function. For systems in a harmonic trap, Ω_l can be well approximated as $\Omega_l = \Omega e^{il\phi}$, where $\Omega = \Omega_R e^{-q^2\bar{\sigma}^2/4}$ and $\phi = qd$ [37], with $\bar{\sigma}$ the average σ_l defined in Eq. (10) and d the mean particle distance $d = \overline{\bar{x}_{l+1} - \bar{x}_l}$. Such an approximation is justified by noting that σ_l and $\bar{x}_{l+1} - \bar{x}_l$ differ little between different i, as shown in Table I. Finally we arrive at the following effective Hamiltonian for SOC:

$$H_{\rm SOC} = -\frac{\Omega}{\sqrt{2}}\sum_{l=1}^{N}(e^{il\phi}s_{l-} + \text{H.c.}). \quad (60)$$

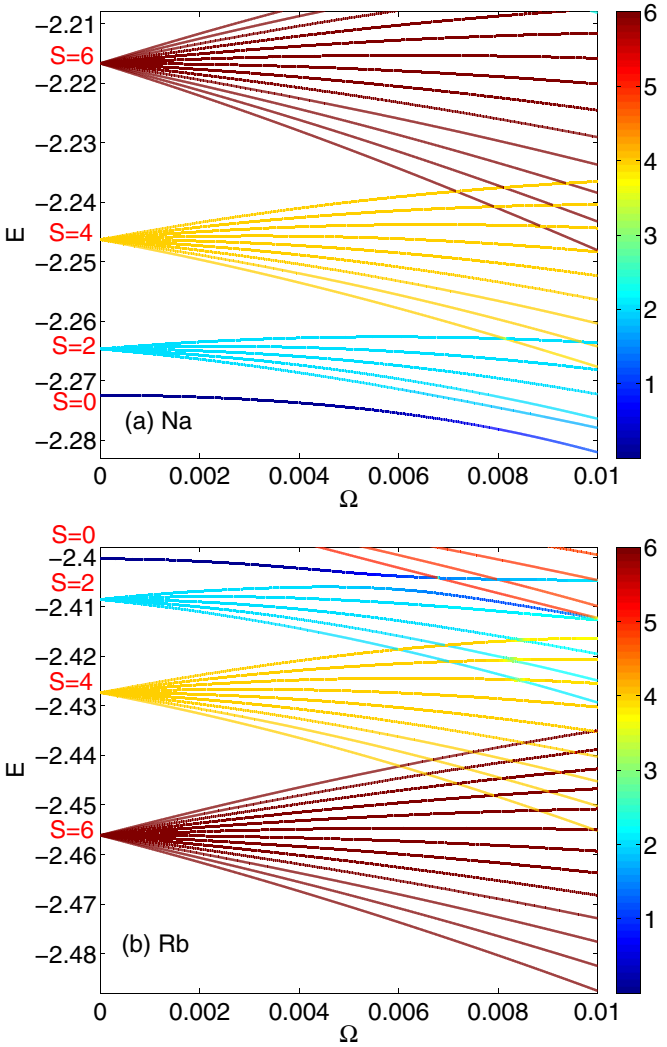

FIG. 2. Energy spectrum as a function of spin-orbit coupling strength Ω for (a) ^{23}Na and (b) ^{87}Rb atoms with a total number of particles $N = 6$. Different colors represent different spin values determined by $S(S+1) \equiv \langle\mathbf{S}^2\rangle$. Here ϕ is chosen to be $\pi/4$. All energies are in the unit of C_N/g_0; g_0/g_2 is 1.05 for ^{87}Rb and 0.95 for ^{23}Na.

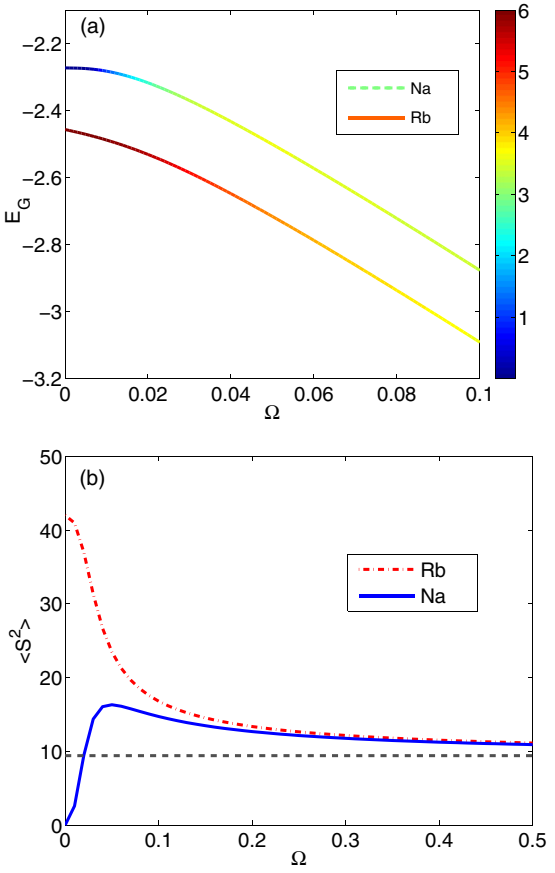

FIG. 3. (a) Ground-state energy E_G and (b) total spin $\langle \mathbf{S}^2 \rangle$ as a function of Ω for both ^{23}Na and ^{87}Rb. The gray dashed line in (b) shows the universal value in the SOC-dominated regime. All parameters and units are the same as in Fig. 2.

Note that here, as we are limited at small Ω_R ($\ll \omega_T$) and moderate $\phi = qd$, we have neglected the contribution from higher-harmonic levels and thus the extra spin-exchange terms as pointed out in Ref. [38].

In Fig. 2 we show the energy spectrum as a function of Ω for both ^{23}Na ($g_0 < g_2$) and ^{87}Rb ($g_0 > g_2$) systems with particle number $N = 6$ and rotation angle $\phi = \pi/4$. In the absence of SOC ($\Omega = 0$), the total spin is conserved. For ^{23}Na, the ground state is a singlet with $S = 0$ and as S increases the energy also increases. For ^{87}Rb, the situation is reversed: The ground state is highly degenerate with the largest total spin $S = N = 6$ and the energy increases as S decreases. For both ^{23}Na and ^{87}Rb, we can see that the states are degenerate for different magnetization M with the same S. However, this is no longer true when the SOC strength is even slightly increased ($\Omega > 0$). In this case, the original degeneracies are completely lifted, as shown by Figs. 2(a) and 2(b), because the SOC field in (60) does not commutate with the total spin.

In Fig. 3 we show the ground-state energy E_G and $\langle \mathbf{S}^2 \rangle$ as a function of Ω. We see that E_G of both ^{23}Na and ^{87}Rb decrease with increasing Ω, while the total spin tends to approach the same value at $\Omega \geqslant 0.4 C_N/g_0$. In this regime, the AFM or FM correlation in the spin-chain model is fully destroyed by the SOC field and the systems of both ^{23}Na and ^{87}Rb are fully governed by the local rotating field in $H_{\rm SOC}$ [Eq. (60)]. Thus

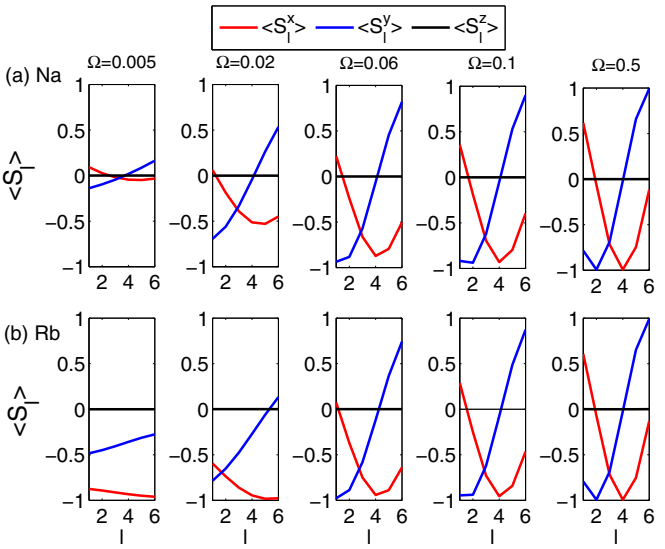

FIG. 4. Local spin $\langle \mathbf{s}_l \rangle$ in the ground state at several values of Ω for (a) ^{23}Na and (b) ^{87}Rb atoms. All parameters and units are the same as in Fig. 2.

increasing Ω, the system will undergo a crossover from the interaction-dominated to the SOC-dominated regime.

One can also see the evidence of such a crossover by examining the spin structure and the contact of the system. Figures 4–6 show, respectively, the spin texture $\langle \mathbf{s}_l \rangle$, nearest-neighbor correlation $\langle \mathbf{s}_l \cdot \mathbf{s}_{l+1} \rangle$, and the contacts $C_\alpha = \partial E_G / \partial g_\alpha^{-1}$ ($\alpha = 0,2$) for the ground states of ^{23}Na and ^{87}Rb at several values of Ω. At zero or small Ω, we can see clearly the signature of AFM or FM correlations: For ^{23}Na, $\langle \mathbf{s}_l \rangle \sim 0$ for all i characterizing the polar or nematic ground state; for ^{87}Rb, we have $|\langle \mathbf{s}_l \rangle| \sim 1$ for all i, $\langle \mathbf{s}_l \cdot \mathbf{s}_{l+1} \rangle = 1$ for any nearest-neighbor pair, and $C_0 = 0$ all characterizing a FM state. With increasing Ω, both ^{23}Na and ^{87}Rb will develop a large spin spiral with

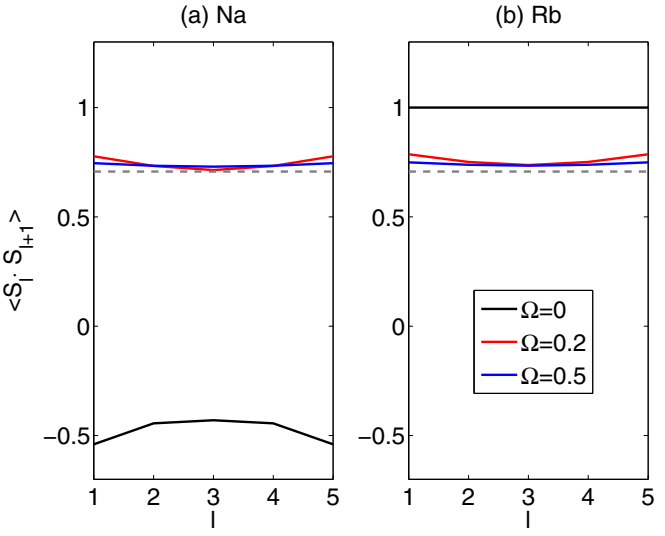

FIG. 5. Spin-spin correlation $\langle \mathbf{s}_l \cdot \mathbf{s}_{l+1} \rangle$ in the ground state at several values of Ω for (a) ^{23}Na and (b) ^{87}Rb atoms. Gray dashed lines show the universal value in the SOC-dominated regime. All parameters and units are the same as in Fig. 2.

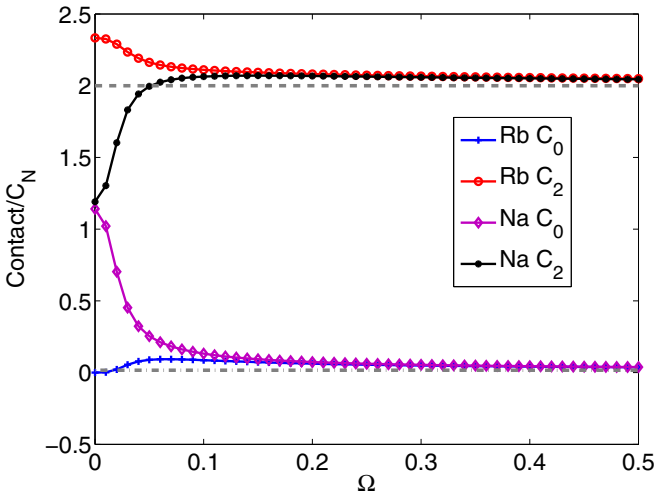

FIG. 6. Contact C_α ($\alpha = 0,2$, in the unit of C_N) for the ground state as a function of Ω for ^{23}Na and ^{87}Rb atoms. Gray dashed lines show the universal values in the SOC-dominated regime. All parameters and units are the same as in Fig. 2.

amplitude of the order of unity (see Fig. 4). Consequently, $\langle \mathbf{s}_l \cdot \mathbf{s}_{l+1} \rangle$ and C_α also approach universal values for both ^{23}Na and ^{87}Rb, which do not change as Ω increases further (see Figs. 5 and 6). When at the special point of infinite coupling, any infinitesimal Ω will induce a large and universal spin spiral, as identified previously in the spin-$\frac{1}{2}$ fermion case [37].

In the SOC-dominated regime, each site l in the spin-chain model (52) is decoupled from each other and the ground state can be straightforwardly obtained as

$$|\Psi_G\rangle = \prod_l \frac{1}{2}(e^{il\phi}c^\dagger_{l,1} - \sqrt{2}c^\dagger_{l,0} + e^{-il\phi}c^\dagger_{l,-1})|\text{vac}\rangle, \quad (61)$$

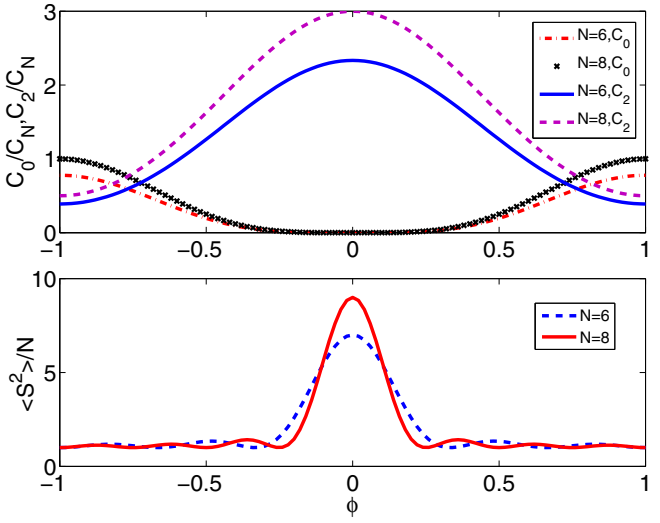

FIG. 7. Shown on top are the contacts C_0, C_2 (in the unit of C_N) and on bottom the total spin $\langle S^2 \rangle / N$ as functions of rotation angle ϕ (in the unit of π) for the ground states of $N = 6,8$ particles in the SOC-dominated regime.

where $c^\dagger_{l,m}$ is the creation operator of a single atom with magnetic number m at site l. Given the wave function (61), we can get the following universal physical quantities:

$$\langle \mathbf{s}_l \rangle = [\cos(l\phi), \sin(l\phi), 0], \quad (62)$$

$$\langle \mathbf{s}_l \cdot \mathbf{s}_{l+1} \rangle = \cos\phi, \quad (63)$$

$$\langle \mathbf{S}^2 \rangle = N + \sin^2(N\phi/2)/\sin^2(\phi/2), \quad (64)$$

$$C_0/C_N = \left(\frac{1}{12} - \frac{1}{6}\cos\phi + \frac{1}{12}\cos^2\phi\right)\sum_l j_l, \quad (65)$$

$$C_2/C_N = \left(\frac{13}{24} + \frac{5}{12}\cos\phi + \frac{1}{24}\cos^2\phi\right)\sum_l j_l. \quad (66)$$

From Figs. 3–6 we can see that these universal values fit the numerical results well in the SOC-dominated regime (with fixed ϕ and N). In Fig. 7 we further show how these universal values of the contacts and the total spin depend on the rotation angle ϕ for six and eight particles.

IV. SUMMARY

We have presented a general form of effective spin-chain model for strongly interacting 1D trapped systems, which is applicable for an arbitrary spin, any statistics (Bose or Fermi), and any spin-independent confinement potentials. Importantly, this general model, as shown in Eq. (49), contains two essential ingredients. One is the local coupling parameter due to the inhomogeneity of charge density in the trapped system, which is irrelevant to spins. The other is the nearest-neighbor spin projection, which generically follows the same structure as the interaction models and uniquely determines the spin-spin correlation and magnetic property of the system. Such an effective model reflects the intrinsic relation between the statistics, scattering channels, and the nature of the ground state. It can serve as a useful and efficient tool to study the equilibrium and nonequilibrium properties of strongly interacting 1D trapped systems.

Taking the spin-1 bosons as an example, we further showed how the addition of spin-orbit coupling can destroy the original magnetic property according to the effective spin-chain model. Increasing the SOC strength, the system undergoes a crossover from the interaction-dominated regime to the SOC-dominated regime and eventually a ground state with universal spin structure and contacts will be achieved. Here the spin-chain model allows the study of the interplay between strong-interaction, high-spin, and spin-orbit coupling in a convenient and physically transparent manner.

ACKNOWLEDGMENTS

We would like to thank Nikolaj T. Zinner for helpful feedback on the manuscript. This work was supported by the National Natural Science Foundation of China under Grants No. 11374177, No. 11421092, and No. 11534014 and the programs of the Chinese Academy of Sciences.

[1] M. D. Girardeau, J. Math. Phys. (N.Y.) **1**, 516 (1960).
[2] M. D. Girardeau and A. Minguzzi, Phys. Rev. Lett. **99**, 230402 (2007).
[3] F. Deuretzbacher, K. Fredenhagen, D. Becker, K. Bongs, K. Sengstock, and D. Pfannkuche, Phys. Rev. Lett. **100**, 160405 (2008).
[4] L. Guan, S. Chen, Y. Wang, and Z.-Q. Ma, Phys. Rev. Lett. **102**, 160402 (2009).
[5] M. D. Girardeau, Phys. Rev. A **82**, 011607(R) (2010).
[6] B. Paredes, A. Widera, V. Murg, O. Mandel, S. Folling, I. Cirac, G. V. Shlyapnikov, T. W. Hansch, and I. Bloch, Nature (London) **429**, 277 (2004).
[7] T. Kinoshita, T. Wenger, and D. S. Weiss, Science **305**, 1125 (2004).
[8] E. Haller, M. Gustavsson, M. J. Mark, J. G. Danzl, R. Hart, G. Pupillo, and H. C. Nägerl, Science **325**, 1224 (2009).
[9] F. Serwane, G. Zürn, T. Lompe, T. B. Ottenstein, A. N. Wenz, and S. Jochim, Science **332**, 336 (2011).
[10] G. Zürn, F. Serwane, T. Lompe, A. N. Wenz, M. G. Ries, J. E. Bohn, and S. Jochim, Phys. Rev. Lett. **108**, 075303 (2012).
[11] A. N. Wenz, G. Zürn, S. Murmann, I. Brouzos, T. Lompe, and S. Jochim, Science **342**, 457 (2013).
[12] X. Cui and T.-L. Ho, Phys. Rev. Lett. **110**, 165302 (2013).
[13] X. Cui and T.-L. Ho, Phys. Rev. A **89**, 023611 (2014).
[14] E. H. Lieb and D. Mattis, Phys. Rev. **125**, 164 (1962).
[15] E. Eisenberg and E. H. Lieb, Phys. Rev. Lett. **89**, 220403 (2002).
[16] K. Yang and Y. Q. Li, Int. J. Mod. Phys. B **17**, 1027 (2003).
[17] K. A. Matveev and A. Furusaki, Phys. Rev. Lett. **101**, 170403 (2008).
[18] X.-W. Guan, M. T. Batchelor, and J.-Y. Lee, Phys. Rev. A **78**, 023621 (2008).
[19] X.-W. Guan, M. T. Batchelor, and M. Takahashi, Phys. Rev. A **76**, 043617 (2007).
[20] S. E. Gharashi and D. Blume, Phys. Rev. Lett. **111**, 045302 (2013).
[21] P. O. Bugnion and G. J. Conduit, Phys. Rev. A **87**, 060502(R) (2013).
[22] T. Sowiński, T. Grass, O. Dutta, and M. Lewenstein, Phys. Rev. A **88**, 033607 (2013).
[23] E. J. Lindgren, J. Rotureau, C. Forssén, A. G. Volosniev and N. T. Zinner, New J. Phys. **16**, 063003 (2014).
[24] F. Deuretzbacher, D. Becker, J. Bjerlin, S. M. Reimann, and L. Santos, Phys. Rev. A **90**, 013611 (2014).
[25] A. G. Volosniev, D. V. Fedorov, A. S. Jensen, M. Valiente, and N. T. Zinner, Nat. Commun. **5**, 5300 (2014).
[26] L. Yang, L. Guan, and H. Pu, Phys. Rev. A **91**, 043634 (2015).
[27] J. Levinsen, P. Massignan, G. M. Bruun, and M. M. Parish, Sci. Adv. **1**, e1500197 (2015).
[28] S. Murmann, F. Deuretzbacher, G. Zürn, J. Bjerlin, S. M. Reimann, L. Santos, T. Lompe, and S. Jochim, Phys. Rev. Lett. **115**, 215301 (2015).
[29] A. G. Volosniev, D. Petrosyan, M. Valiente, D. V. Fedorov, A. S. Jensen, and N. T. Zinner, Phys. Rev. A **91**, 023620 (2015).
[30] P. Massignan, J. Levinsen, and M. M. Parish, Phys. Rev. Lett. **115**, 247202 (2015).
[31] Y. J. Lin, R. L. Compton, K. Jimnez-Garca, J. V. Porto, and I. B. Spielman, Nature (London) **462**, 628 (2009); Y.-J. Lin, K. Jimnez-Garca, and I. B. Spielman, *ibid.* **471**, 83 (2011).
[32] J.-Y. Zhang, S.-C. Ji, Z. Chen, L. Zhang, Z.-D. Du, B. Yan, G.-S. Pan, B. Zhao, Y.-J. Deng, H Zhai, S. Chen, and J.-W. Pan, Phys. Rev. Lett. **109**, 115301 (2012); J.-Y. Zhang, S.-C. Ji, L. Zhang, Z.-D. Du, W. Zheng, Y.-J. Deng, H. Zhai, S. Chen, and J.-W. Pan, Nat. Phys. **10**, 110 (2014).
[33] P. Wang, Z. Q. Yu, Z. Fu, J. Miao, L. Huang, S. Chai, H. Zhai, and J. Zhang, Phys. Rev. Lett. **109**, 095301 (2012); Z. Fu, L. Huang, Z. Meng, P. Wang, L. Zhang, S. Zhang, H. Zhai, P. Zhang, and J. Zhang, Nat. Phys. **10**, 110 (2014).
[34] L. W. Cheuk, A. T. Sommer, Z. Hadzibabic, T. Yefsah, W. S. Bakr, and M. W. Zwierlein, Phys. Rev. Lett. **109**, 095302 (2012).
[35] R. A. Williams, M. C. Beeler, L. J. LeBlanc, K. Jimenez-Garcia, and I. B. Spielman, Phys. Rev. Lett. **111**, 095301 (2013).
[36] C. Qu, C. Hamner, M. Gong, C. Zhang, and P. Engels, Phys. Rev. A **88**, 021604(R) (2013).
[37] X. Cui and T.-L. Ho, Phys. Rev. A **89**, 013629 (2014).
[38] Q. Guan and D. Blume, Phys. Rev. A **92**, 023641 (2015).
[39] M. Olshanii, Phys. Rev. Lett. **81**, 938 (1998).
[40] The spreading property will crucially depend on the type of underlying trapping potential. Other potentials will have different properties [29, 41].
[41] O. V. Marchukov, E. H. Eriksen, J. M. Midtgaard, A. A. S. Kalaee, D. V. Fedorov, A. S. Jensen, and N. T. Zinner, arXiv:1508.07164.
[42] M. Barth and W. Zwerger, Ann. Phys. (Amsterdam) **326**, 2544 (2011).
[43] H. Hellmann, *Einfhrung in die Quantenchemie* (Deuticke, Leipzig, 1937), p. 285; R. P. Feynman, Phys. Rev. **56**, 340 (1939).
[44] N. T. Zinner (private communication).
[45] T.-L. Ho and S. K. Yip, Phys. Rev. Lett. **84**, 4031 (2000).
[46] S. Tuchiya and S. Kurihara, J. Phys. Soc. Jpn. **70**, 1182 (2001).
[47] S. K. Yip, Phys. Rev. Lett. **90**, 250402 (2003).
[48] A. Imambekov, M. Lukin, and E. Demler, Phys. Rev. A **68**, 063602 (2003).
[49] S. Tsuchiya, S. Kurihara, and T. Kimura, Phys. Rev. A **70**, 043628 (2004).